International Journal of Advanced Technology in Engineering and Science
Vol. No.3, Issue 11, November 2015
www.ijates.com
ijates
ISSN 2348 - 7550

EXPERIMENTAL TECHNIQUE TO EVALUATE THE NANOMECHANICS AT NANOSCALE OF CARBON NANO TUBES

Upendra Sharan Gupta[1], Rahul Singh [2], Savan Parmar[3], Prasanna Gupta[4]

[1]Reader, [2,3,4] UG Scholar, Dept. of Mech. Engineering, SVITS, Indore, (India)

ABSTRACT

The impact of the nanotechnologies on the everyday life issues is not only restricted to the application of the scientific discoveries, but also concerns the exploration of the fundamental processes and interactions that take place in the matter at the atomic level. Nanomaterials are perfect representations of one-, two-, or three-dimensional objects in their simplest forms. It becomes then possible to compare their real behavior when varying parameters such as stresses, electric or magnetic fields, with precise numerical simulations based on the actual laws of physics. This kind of comparisons between experiments and theory on low dimension objects is helpful to better understand the interactions at the atomic scale. Thus, nanomaterials represent one of the most rapidly expanding and challenging fields of research that crosses many borders between areas of natural sciences and physics. This paper related to the behavior of nanometer sized structures under stress and strain compared to our knowledge for the same geometries at larger scale. This paper describes the Experimental Technique to evaluate the Nano mechanics at nanoscale of carbon Nano tubes .This paper describes the mechanics of carbon nanotubes. In order to stay in the linear elasticity regime, small indentation amplitudes have been applied in the radial direction of multi walled carbon nanotubes adsorbed on a silicon oxide surface.

Keywords: Nano Tribology, Nano Mechanics, Carbon Nanotube

I. INTRODUCTION TO NANOSTRUCTURED MATERIALS

Nanostructures usually refer to structured devices with a size of few nanometers to several hundreds of nanometers. E.g. cell components or viruses, extremely small sand grains or nonmetric droplets of water. Nanostructures are further classified into inorganic nanostructures and organic nanostructures [1].**Inorganic nanostructures:** A well-known group of inorganic nanostructures is the fullerenes. They are part of the allotropes of the carbon, one of the most important elements in nature. The fullerenes [2] introduced new stable carbon structures in the form of hollow spheres called Bucky balls or buckminsterfullerene, onion-like graphitic sphere tubes called carbon nanotubes [3]. **Nanotubes** find their application in a wide range of techniques such as components of Nano electronic devices like field-effect transistors, and are also good components for mechanically reinf orced composite materials and nanometer sized sensors.

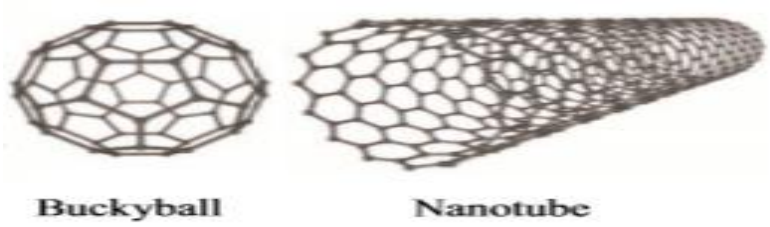

Fig. 1

The potential of applications of the nanotubes led to the development of other kinds of small cylindrical shaped Nano-objects: the **nanowires** (also called **Nano rods**). These Nano objects, essentially based on metallic elements, are wire-like nanomaterials, such as carbides[4] , nitrides[5], oxides[6,7] , having as common characteristic a cylindrical symmetric cross-section.

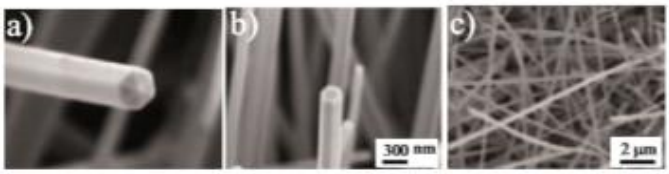

Fig. 2

Example of nanowires: (a) and (b) are hexagon and pentagon shaped ZnO nanowires, whereas (c) presents GaN nanowires.

Another two-dimensional nanostructure is the **nanobelt [8]**. Nano belts are made of different semiconducting oxides, like zinc or tin, and are synthesized by evaporating metal oxide powders at high temperatures. One of their distinctive features is to be an ideal system for understanding piezoelectric effect and spontaneous polarization induced ferroelectric effect at the nanoscale.

Finally, numerous inorganic nanostructures show potential applications as one-dimensional nanoscale sensors, transducers, resonators or lasers [9, 10, and 11].

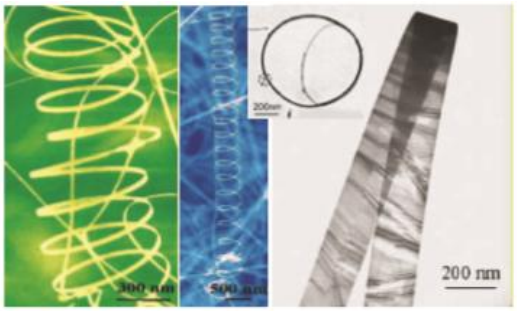

Fig. 3: Nano Belts in the Form of Springs, Rings and Ribbon

II. ORGANIC NANOSTRUCTURES

The organic nanostructures are chemical compounds consisting primarily of carbon and hydrogen. They are extremely flexible in being tailored to meet the needs of particular applications. They show great potential for coating and molding as well as their production cost is also low. Nanostructured organic thin films are used as organic light emitting devices (OLEDs) and also as organic thin film transistors. [12, 13, 14]

III. MECHANICS OF NANOSTRUCTURES

In this section, we discuss the two methods and related theories used for measuring the mechanical properties of the CNTs. Both the methods rely on atomic force microscopy. The AFM technique has already been used to characterize numerous organic and inorganic nanostructures. Among the inorganic nanostructures, a pronounced interest was shown for tubular nanostructures and long thin structures, such as CNTs, ropes of CNTs, Nano belts and nanowires, which have an adequate symmetry and shape for experimental manipulations and theoretical calculations. The faculty of the AFM to work in different kinds of surrounding environments, like in liquids, has also led to its common use for probing biological samples, among which we find the T4 bacteriophages on silicon substrates, pox viruses and living cells, microtubules, and finally, the Nano indentation of viral capsids to determine how the strength and elasticity depend on the capsid structure. Thus, the versatility and easy use of the AFM make it the ideal tool to test materials at the nanoscale under different working environments. [19]
Another interesting alternative method to the AFM is based on nanostructures resonance using TEM. It has been used to characterize the elasticity of CNTs and nanowires, and also Nano belts [24]. In each case, the obtained values agreed with the AFM results. Unfortunately, it is sometimes subject to large errors bars (20-60%) and it cannot be applied in a way as general as the AFM techniques. It needs effectively special preparation of the Nano-objects for the vacuum and it tests almost only the bending elastic property of long thin structures. [20, 21, 23]

IV. THE MODULATED NANO INDENTATION AFM METHOD

In this technique, the amplitude of the oscillations is chosen very small, close to 1 Å, in order to remain in the sticking and elastic regime of the tip interacting with the Nano-object surface. In this amplitude range and experimental geometry, the normal force FN required to move vertically the support of the Nano-object by a distance D with respect to the cantilever support coincides with the force needed to elastically stretch two springs in series the cantilever, with stiffness knead the tip sample contact, with stiffness kcont. If D is the total normal displacement of the Nano-object support, i.e., D is equal to cantilever bending plus tip and Nano-object normal deformation, and FN is the total normal force, then this configuration allows the measurement of the total stiffness ktot at each load, defined by the relation:

$$dFN / dD = ktot = (1/kN + 1/kcont)^{-1} \ldots\ldots (1)$$

Since kN is known, a measurement of dFN/dD at different normal loads leads to the value of kcont as a function of FN. For this, a lock-in amplifier is used to vertically modulate the Nano-object support, dD, and measure dFN. Figure illustrates the experimental results of the normal modulated Nano indentation method applied to a CNT. It gives access simultaneously to the topography, the friction force and the total stiffness of the system while scanning the surface.

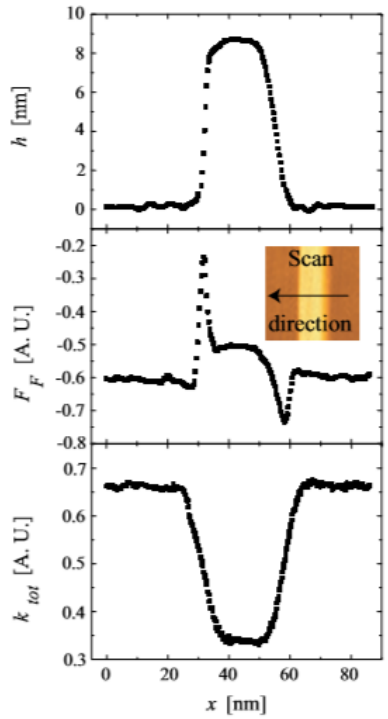

Fig.4: Illustration of the normal modulated Nano indentation technique on a multiwall CNT adsorbed on a silicon oxide surface. This technique allows to record simultaneously the topography h, the friction force FF, and the total stiffness of the system as function of the AFM tip displacement x.

We can extract then the related Young modulus E from kcont versus FN measurements by modelling the contact between the AFM tip and the Nano-object, here a CNT, with the Hertz model [23]. We underline that the extracted E is therefore the linear elasticity of the object under a stress normal to its surface. Thus, under the assumptions of standard elasticity theory, the Hertz model gives the dependence of the indentation distance δz versus the normal force FN between two elastic solids in contact. Although very sophisticated extensions of this model were developed to include the effect of the adhesion at low external forces, in the context of this work, it suffices to use the first level approximation, consisting of an additive correction of the normal force FN . We consider the contact between a sphere and a cylinder (corresponding to the tip and the CNT) of respective radii RT and Rcyl, and we include the adhesive force Fadh, which is experimentally determined.

$$Kcont = 1/Cz = \beta[R(FN + Fadh)/K^2]^{1/} \quad ....(2)$$

$$1/R = 1/Rr + 1/Rcyl$$

$$K = 3/4\ [(1-\nu1^2)/E1 + (1-\nu2^2)/E2\ ] \quad ...(3)$$

$$\beta = (\pi/2k)^{2/3}.\ E[(\sqrt{1-k^2})]^{1/3}/K(\sqrt{1-k^2}) \quad ...(4)$$

Where ν1, ν2 and E1, E2 are respectively the Poisson ratios and radial Young moduli of the sphere and the cylinder. For convenience, we put in β the parameters related to the geometry of the contact area Thus, by fitting kcont versus FN , we obtain the radial Young modulus E2 = Erad of the cylindrical nanostructure, as it is the only free fit parameter.

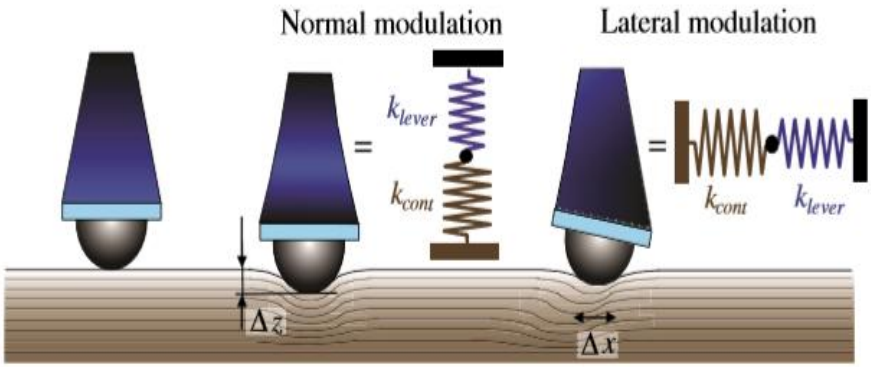

Fig.5: Sketch of the normal and lateral surface stiffness measurement while indenting a surface. The total stiffness is represented by two springs in series, klever and kcont being respectively the elastic constants of the tip-cantilever and the probed surface.

V. CLASSICAL ELASTIC BEAM IN THE NANO WORLD

Another interesting method that gives access to the mechanical properties of high aspect ratio nanostructures is based on the classical elastic beam. It consists in measuring the normal deflection d(y) of a suspended Nano beam under the assumption of clamped beam. This method has already been used to measure the bending Young modulus of CNTs [22] and microtubules [25] submitted to a normal force FN loading the middle of the suspended length. In our case, we will not be restricted to a single normal force FN applied to the middle of the beam, but we will consider a discrete gradient *f(y)* of forces *Fi* applied along the whole length of the beam. .Moreover, the geometric configuration of the problem leads to choose the case of a symmetric gradient of force *f(y)* relatively to the center of mass of the beam. It represents for example the action of the vdW forces between the Nano beam and its surrounding environment.

We consider now a beam with its long axis a long *y* and of suspended length L. The discrete division $dy = yi - yi-1$ of the beam along the y-axis is given by the equation $dy = (L - 2h)/N$ where N is a positive entire multiple of 2, representing the number of divisions of the TMV and chosen so that $dy \sim = 0.4\ nm$. The parameter *h* takes into account the RMS roughness of the surface on which the Nano beam lies. Each force *Fi (i =1, N)* composing the discrete gradient *f(y)* is directed along z, perpendicularly to the y-axis. As the loading forces *Fi* are symmetric compared with the midpoint of the beam, the reaction forces Ry and moments *my* acting in $y = 0$ and $y = L$ are equal: $R0 = RL$ and $M0 = ML$. Moreover, it results from Newton's equations projected along the z-axis at the static equilibrium that, R0, z = RL, z = ½ $\sum Fi$, where we considered that the forces *Fi* are negative.

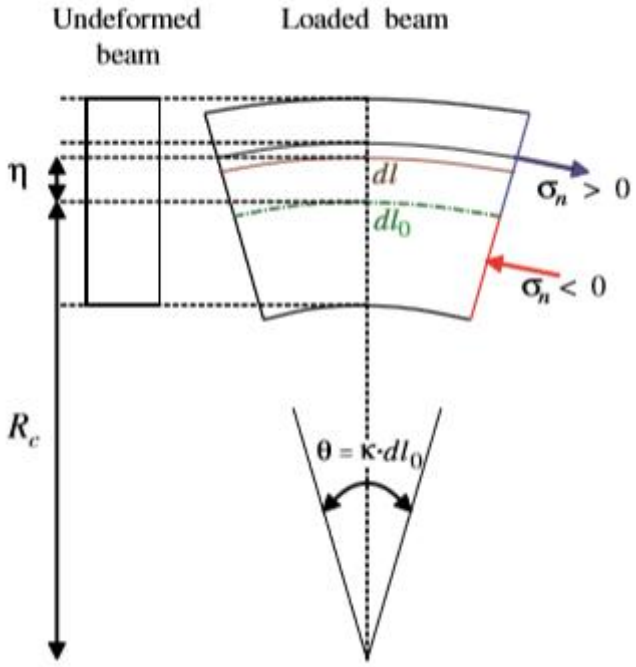

Fig.6 Representation of the Stress-Strain on a Loaded Beam

According to the beam theory, the upper and lower part of the beam will be alternatively in tension and in compression, submitted to a stress σn. While the lower part of the beam is in compression (σn < 0), the upper part is in tension (σn > 0) and vis versa. Inside the beam, there is a surface that does not change in length, called the neutral surface of the beam which is represented by *dl0*. It is the line of zero normal strain. For a beam made of a material that obeys the Hooke's law, this surface will pass through the middle of the beam. Referring to Fig.6 and taking the origin of the η-coordinate axis at the neutral surface, the stress distribution is given by

$$\sigma_n = E.\varepsilon_n = E.\ (dl_o - dl)/\ dl_o \ldots..(5)$$

$$= E.\ [(R_c+\eta)\theta - R_c.\theta]/\ R_c.\theta$$

$$= E.\eta/R_c \ldots(6)$$

Where εn is the normal strain distribution, Rc is the radius of curvature of the neutral surface and E is the bending Young modulus of the beam. Then, the bending moments M due to the stress acting on a small beam section positioned arbitrarily in y = a is given by

$$M = \int_{section} \eta\ \sigma_n.dS \qquad \ldots(7)$$

$$= E/R_c \int_{section} \eta^2 dS = EI/R_c$$

$$= \kappa EI \qquad \ldots.(8)$$

Where κ =1/Rc is the beam curvature and I is the inertial momentum of the section of the beam along its long axis. In the case of a cylindrical beam of diameter D, we have $I = D^4/64$. This total bending moment is also equal to the sum of the bending moments due to the forces acting on the beam for *y>a*. Applying these last considerations in our case, we have for $y_{i-1} + dy/2 \geq a$.

$$EI / R_c = \sum F_i\ .\ (\ y_{i-1} + dy/2 - a\ ) - M_L + R_L\ .\ (L-a) \ldots\ldots..(9)$$

For small deformations, the deflection *d(y)* of the beam relatively to its non-deformed position is related to the curvature of the neutral surface via simple geometric considerations. At the first order, the relationship between κ and *d(y)* becomes

$$k = 1 / R_c = d^2d(y)/dy^2 \ldots\ldots\ldots (10)$$

Finally, by combining the above two equations, we obtain for yi-*1 + dy/2* $\geq y = a$

$$EI.d^2d(y)/dy^2 = \sum F_i \,.\, (y_{i-1} + dy/2 - y) - M_L + R_L \ldots\ldots.(11)$$

The double integration of this last equation versus y under the boundary conditions of clamped beam and continuity gives rise to the suspension depth *d(y)* for *0 <y<L*. The maximum suspension depth is then found at the middle of the Nano beam, corresponding to *d (L/2).* This last formula gives a direct access to the bending Young modulus *E* from experimental measurements of the suspended beam geometry once the forces acting on the beam have been determined

VI. THE MULTIWALL CARBON NANOTUBE

The first part of this section [3] provides a concise review of the main characteristics of the CNTs, while the second part focuses more deeply on their mechanical properties to finally present our experimental results on the radial Young modulus of multiwall CNTs.

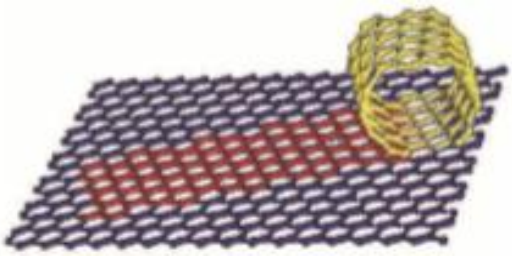

Fig. 7: Each layer forming a CNT is analog to a graphene sheet wrapped seamlessly onto itself.

VII. DESCRIPTION AND CHARACTERISTICS

Multi walled carbon nanotubes (MWCNTs) [3] are part of the fullerenes. They consist of grapheme sheets wrapped seamlessly onto themselves forming a tube of concentric shells with an outer diameter ranging from 1 to 50 nm for lengths up to several micrometers.

7.1 CNTs Chirality

There are different manners to form a cylinder with a sheet of graphene, resulting finally in one concentric layer of a CNT. If the plane is rolled up along one of the symmetry axis of the graphite, it gives either a zig-zag tube or an armchair tube. It is also possible to roll up the sheet in a direction that differs from a symmetry axis. The obtained CNT is then called a chiral nanotube. The chirality of the CNTs influences its properties. For example, depending on the chirality, the tube is either metallic or semi conductive.

7.2 Synthesis of CNTs:

There are three main procedures for the synthesis of CNTs. They are the chemical vapor deposition (CVD), the arc discharge (AD) method and the laser ablation (LA) method. The quantity, the quality and the characteristics

of the tubes obtained with these different methods vary slightly. The CVD technique is the more flexible method, producing a high quantity of CNTs, but sometimes with a non-negligible amount of defects. The AD method generates a mixture of fullerenes which requires different procedures of purification to differentiate the CNTs. The LA method produces high quality CNTs, but in very small quantities.

7.3 CVD

The CVD is based on chemical vapor deposition . It consists in chemical reactions that take place in a tube furnace and transform gaseous molecules of hydrocarbon flowing into the tube into solid material on the surface of a substrate prepared with a layer of catalyst particles of transition metal.

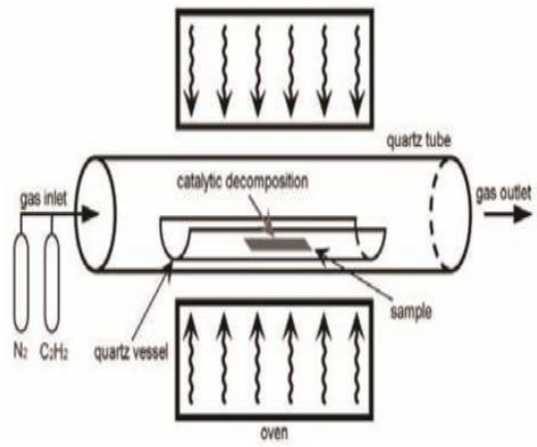

Fig. 8: The CVD method: Chemical reactions transform the gaseous molecules into the CNT solid material. The decomposition of the gas ($C_2H_2 \rightarrow C_2 + H_2$ in the case of acetylene) and the nanotube growth are activated by the catalyst, which usually is iron, cobalt or nickel. The oven is typically working at temperature of~700◦C. On one end of the tube, the gases are introduced and at the other end, they are pumped out by a vacuum pump.

7.4 AD Method

The arc discharge method was initially used for producing C60 fullerenes and then to manufacture CNTs . It is based on the cooling of carbon plasma generated by an electric arc discharge between two graphite rods (electrodes).The carbonize vaporated by a plasma of inert gas in a confined environment in which are placed the two electrodes. The gases are usually helium, argon or hydrogen at pressure from 50 to 900 mbar. Due to the high current density between the electrodes, and thus, high temperature, the rods gently evaporate, while the distance between them is kept constant . At the end, upon cooling, a soot containing the fullerenes is collected on the cathode.

7.5 LA Method

The laser ablation method consists in intense laser pulses that are used to ablate a carbon target placed in a furnace heated at 1200◦C . Then, during the laser ablation process, a flow of inert gas passing inside the furnace

carries the produced CNTs that arecollectedon a cold collector. This method produces a majority of CNT bundles.

VIII. MOLECULAR DYNAMICS SIMULATIONS

To mimic the experiments, molecular dynamics (MD) simulations with empirical C−C potentials have also been performed by modelling the AFM tip as a rigid continuous sphere and the CNT by atoms interacting through an empirical potential. For this, forces between carbon atoms are derived from a two-body pair energy plus a three-body angular penalty for the covalent energy (intra-layer energy), as developed by N.A.Marks and from a truncated Lennard-Jones potential for the inter-layer energy, as applied by J. P. Lu. Subsequently, the CNTs are compressed between the rigid sphere and a rigid plane using short range purely repulsive potentials for both interactions. The two ends of the CNTs are frozen. The CNT length and the sphere radius are respectively fixed to 20 and 12nm.

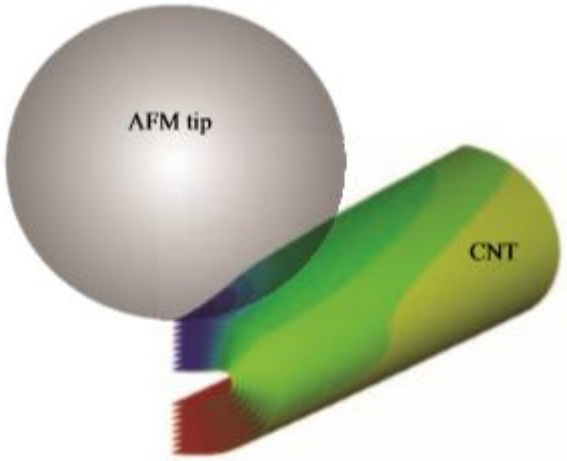

Fig. 10: Simulation of the Indentation of a MWCNT by a Rigid Sphere Representing the AFM tip.

IX. CONCLUSION

This Paper deals with the continuum mechanics applied to small tubular structures in order to evaluate their elastic properties. The diversity and the fabulous potential of applications of the the nanostructures is briefly reviewed by presenting some advances in nanotechnologies. Then, theoretical models based on continuum mechanics are developed to mimic the elastic behavior of tubular nanostructures. Finally, these models are applied to AFM measurements of the elastic deformations of hard carbon nanotubes. For many fields of the nanotechnologies, we are more observers than actors, still being surprised by the ability of the nature in synthesizing fine and elegant nanostructures in ambient temperature, while we have to use high pressure and/or high temperature. Nevertheless, the tendency is gently changing. The future developments at an industrial level of Nano-objects with specific physical and chemical properties chosen in function of their applications will probably have a strong economic and social impact on the human being, notably for diseases treatments where nanotechnologies already afford novel techniques such as the intracellular imaging through attachment of

quantum dots or synthetic chromophores to selected molecules .Although wide benefits emerge from the nanotechnologies, we have also to keep in mind that the toxicology of many nanomaterials has not yet been fully evaluated. Thus, while nanotechnology promises many solutions related to health care or energy saving based for example on low weight high strength materials, it remains important to develop at the same time the knowledge of their impact on our environment and for this, it is important to characterize as accurately as possible each nanomaterial.

REFERNCES

[1]. C.-C. You, O. R. Miranda, B. Gider, P. S. Ghosh, I.-B. Kim, B. Erdogan, S. A. Krovi, U. H. F. Bunz, and V. M. Rotello, Nat. Nanotech. 2, 318 (2007).

[2]. H. W. Kroto, J. R. Heath, S. C. O'Brien, R. F. Curl, and R. E. Smalley, Nature 318, 162 (1985).

[3]. S. Iijima, Nature 354, 56 (1991).

[4]. H. Dai, E. W. Wong, Y. Z. Lu, S. Fan, and C. M. Lieber, Nature 375, 769 (1995).

[5]. W. Q. Han, S. S. Fan, Q. Q. Li, B. L. Gu, X. B. Zhang, and D. P. Yu, Appl. Phys. Lett. 71, 2271 (1997).

[6]. P. D. Yang and C. M. Lieber, J. Mat. Res. 12, 2981 (1997).

[7]. Y. Li, G. S. Cheng, and L. D. Zhang, J. Mat. Res. 15, 2305 (2000).

[8]. Z. W. Pan, Z. R. Dai, and Z. L. Wang, Science291, 1947 (2001).

[9]. J. I. Paredes and M. Burghard, Langmuir 20, 5149 (2004).

[10]. K. Balasubramanian and M. Burg hard, Small 1, 180 (2005).

[11]. S. J. Son, X. Bai, A. Nan, H. Ghandehari, and S. B. Lee, J. Control. Release 114, 143 (2006).

[12]. M. Knez, A. Kadri, C. Wege, U. G1osele, H. Jeske, and K. Nielsch, Nano Lett. 6, 1172 (2006).

[13]. A. Dodabalapur, H. E. Katz, L. Torsi, and R. C. Haddon, Science 269, 1560 (1995).

[14]. K. K. W. Wong, T. Douglas, S. Gider, D. D. Awschalom, and S. Mann, Chem. Mater. 10, 279 (1998).

[15]. K. K. W. Wong and S. Mann, Adv. Mater. 8, 928 (1996).

[16]. T. Douglas and M. Young, Nature 393, 152 (1998).

[17]. S. A. Davis, S. L. Burkett, N. H. Mendelson, and S. Mann, Nature385, 420 (1997).

[18]. M. Mertig, R.Wahl, M. Lehmann, P. Simon, and W. Pompe, Eur. Phys. J. D 16, 317 (2001)

[19]. M. Arroyo and T. Belytschko, Meccanica 40, 455 (2005).

[20]. G. Y. Jing, H. Ji, W. Y. Yang, J. Xu, and D. P. Yu, Appl. Phys. A 82, 475 (2006).

[21]. E. W. Wong, P. E. Sheehan, and C. M. Lieber, Science 277, 1971 (1997).

[22]. D. A. Walters, L. M. Ericson, M. J. Casavant, J. Liu, D. T. Colbert, K. A. Smith, and R. E. Smalley, Appl. Phys. Lett. 74, 3803 (1999).

[23]. M. F. Yu, T. Kowaleweski, and R. S. Ruoff, Phys. Rev. Lett. 85, 1456 (2000).

[24]. F.M.Ohnesorge,J.K.H.Horber,W.Haberle,C.-P.Czerny,D.P.E.Smith,andG.Binnig, Biophys. J 73, 2183 (1997).

[25]. A. Kis, S. Kasas, B. Babic, A. J. Kulik, W. Benoît, G. A. Briggs, C. Schoenenberger, S. Catsicas, and L. Forró, Phys. Rev. Lett. 89, 248101 (2002).